

Minimum principles and level splitting in quantum Monte Carlo excitation energies: Application to diamond

M. D. Towler, Randolph Q. Hood,* and R. J. Needs

Cavendish Laboratory, University of Cambridge, Madingley Road, Cambridge CB3 0HE, United Kingdom

(Received 6 December 1999)

A diffusion and variational quantum Monte Carlo (DMC and VMC) study of excitation energies in diamond is reported. Good agreement is found between the DMC results and results from the *GW* approximation and, where available, with experiment. A group theoretical analysis is provided of the level splittings arising from the use of arbitrary degenerate single-particle orbitals in the construction of ground- and excited-state determinants. The results are discussed in light of the recently demonstrated variational theorems for excited states in the DMC study.

I. INTRODUCTION

Quantum Monte Carlo (QMC) methods offer a direct and accurate wave-function-based treatment of quantum many-body effects, and may be used to compute the energy of both ground and excited states of molecules and solids. They are particularly attractive for applications to large systems because the computational cost scales as the cube of the system size, which is highly favorable when compared with other correlated wave-function methods.

A number of QMC techniques have been used for calculating excited state energies. The methods we discuss here are perhaps the most conceptually simple as they involve the construction of a trial wave function to model each excited state. Using such a trial wave function in a variational Monte Carlo¹ (VMC) or fixed-node diffusion Monte Carlo² (DMC) calculation then yields an approximation to the energy of the excited state. This type of method was first used for small molecules³ and more recently has been used for excitation energies in solids.⁴⁻⁶

The trial wave function is central to VMC and DMC methods, as it controls both the statistical variance and the final accuracy obtained. Typically it is taken to be a determinant of single-particle orbitals derived from Hartree-Fock (HF) or Kohn-Sham density functional theory (KS DFT) calculations multiplied by a Jastrow factor that explicitly correlates pairs of particles. Trial wave functions for excited states are formed by modifying the determinantal part of the ground-state trial function. In the calculations reported here we form a trial wave function for an excited state by replacing an occupied orbital in the ground state determinant by a virtual orbital. This corresponds to the physical situation in an optical absorption experiment where an electron is excited from the valence band into the conduction band. Two quasi-particles are introduced into the system, the electron and hole, which interact and form an exciton.

In this paper we use the VMC and DMC methods to study excited states in diamond. We analyze the symmetry of the many-body trial wave functions for the excited states, which is useful in discussing the splitting of the energy levels due to interaction effects and the application of variational theorems to the calculated energies.

II. VARIATIONAL PRINCIPLES FOR EXCITED STATES

For a trial wave function of a definite symmetry the energy calculated within the VMC method is greater than or equal to that of the lowest energy state of that symmetry. The variational principle can be extended to higher excited states by diagonalizing the Hamiltonian in a basis of states linearly independent to exact states of the same symmetry with energies lower than the desired state, which we refer to as the generalized variational theorem.⁷ In practice one can usually obtain reasonable approximations to the energies of higher excited states through the nonvariational procedure of substituting occupied orbitals with the appropriate virtual orbitals in the trial determinant and directly evaluating the VMC energy without orthogonalization to lower energy states. A common procedure is to optimize the Jastrow part of the trial function for the ground state calculation and then to use the same Jastrow factor for the excited states, the trial function differing only in the orbitals making up the determinant. Practical tests have shown that reoptimization in the excited state changes the computed energy by less than the usual statistical error bar of a few hundredths of an eV per atom.

The nature of variational principles within the DMC method is significantly different. If a fixed-node constraint is not imposed on the wave function, propagation of the system in imaginary time does not maintain the fermionic symmetry of the starting state and the solution decays towards the bosonic ground state. This difficulty is a manifestation of the fermion sign problem. Most DMC calculations therefore use the fixed-node approximation,⁸ which for most applications is both accurate and numerically stable. The basic idea is quite simple. The trial many-electron wave function is used to define a many-electron nodal surface. The fixed-node DMC algorithm maintains the nodal surface of the trial wave function, which enforces the fermionic symmetry and produces the lowest energy many-electron wave function consistent with this nodal surface. It is therefore the fixed-node constraint that allows the estimation of excited state energies in DMC calculations.

The nature of variational principles within the fixed-node DMC method was recently explored by Foulkes, Hood, and Needs.⁹ If one models an excited state that is the lowest energy state of a certain symmetry with a trial wave function

without a definite symmetry, there need not be a variational principle for the fixed-node DMC energy. Foulkes, Hood, and Needs⁹ showed that even if one chooses a trial wave function with a definite symmetry, then the resulting fixed-node DMC energy need *not* be above the lowest energy state with that symmetry. Under some circumstances the fixed-node DMC algorithm can break the symmetry of the trial wave function. It turns out that if the trial wave function transforms according to a one-dimensional irreducible representation of the symmetry group of the Hamiltonian, then the fixed-node DMC energy must lie above the energy of the lowest state of that symmetry, but if the irreducible representation is of dimension greater than one, then the fixed-node DMC energy can lie below the exact energy.⁹ Weaker variational bounds may then be obtained by choosing trial functions transforming according to one-dimensional irreducible representations of subgroups of the full symmetry group.

Despite this situation, fixed-node DMC seems to work well as a practical tool for computing excitation energies, even for the higher states of a given symmetry. The reason for this is that the energy of the excited state would be exact if the nodal surface of the trial wave function were exact, so the accuracy of the nodal surface is the key issue. If the nodal surface of the trial function is inexact, then the DMC wave function may not have the same symmetry as the trial function, but the imposed nodal surface acts as such a strong constraint on the DMC wave function that it effectively prevents significant deviations in the energy.

III. LEVEL SPLITTING

The difference between the symmetry group of the Hamiltonian from which the single-particle orbitals are obtained and that of the full interacting Hamiltonian with explicit electron-electron interactions means that a reevaluation of the degeneracy classifications is required. In particular, if the single-particle problem involves the partial filling of localized degenerate energy levels, then one can build a number of different Slater determinants from the degenerate orbitals. If the matrix elements of the interacting Hamiltonian between these Slater determinants are nonzero, then the degeneracy of the states of the single-particle problem will be lifted and we will obtain a multiplet structure. In a situation where the wave function is localized in some sense (e.g., in atoms or isolated point defects) this may be an important effect. In QMC calculations for solids spurious level splitting can occur due to the finite size of the simulation cell. Different choices of single-particle orbitals to describe the wave function of the excited electron and the hole lead to different values of the exciton binding energy. This splitting would disappear in the limit of a large simulation cell but up until now it has not been considered in QMC calculations.

Consider, for example, the direct promotion of an electron across the band gap at the Γ point in diamond (i.e., a $\Gamma_{25'v} \rightarrow \Gamma_{15c}$ optical absorption). In a one-electron ground-state calculation the $\Gamma_{25'v}$ level at the top of the valence band and the conduction band Γ_{15c} level are triply degenerate. A QMC calculation of the energy of this excited state is carried out by replacing one of the valence band orbitals with a conduction band orbital of the same spin in the determinantal part of the trial wave function. This may evidently be done in nine

different ways. Since these nine excited state determinants may consist of different linear combinations of basis functions that transform as different representations of the symmetry group of the many-electron Hamiltonian, there is no reason why they should form a degenerate set, and in general they do not. In fact, no ninefold degenerate irreducible representation exists at the Γ point for any of the 230 space groups.

The precise linear combinations of degenerate single-particle orbitals obtained from our HF or DFT electronic structure code are subject to the whim of the diagonalizer. In the next section the procedure for decomposing this reducible basis into its component irreducible representations (and hence finding the correct linear combinations of determinants that transform according to these irreducible representations) will be demonstrated. It will also be shown that in principle such symmetrized wave functions give the maximum possible level splitting.

IV. GROUP THEORETICAL ANALYSIS

A. Basic ideas

First we consider the relationship between the interacting Hamiltonian \hat{H} used in QMC and the noninteracting Hamiltonian from which the single-particle orbitals are obtained. In the QMC calculation, the infinite crystal is represented by a finite simulation cell subject to periodic boundary conditions. The primitive translation vectors of this supercell are taken to be integer multiples of the primitive translation vectors of the underlying crystal lattice. With these boundary conditions the interacting Hamiltonian can be written as

$$\hat{H} = -\frac{1}{2} \underbrace{\sum_i^N \nabla_i^2 + \sum_i^N v(\mathbf{r}_i)}_{\hat{H}_0 (= \sum_i \hat{H}_0^i)} + \underbrace{\sum_{\mathbf{t}^s} \sum_{i < j}^N \frac{1}{|\mathbf{r}_i - \mathbf{r}_j - \mathbf{t}^s|}}_{\hat{V}_{ee}}, \quad (1)$$

where $\{\mathbf{t}^s\}$ is the set of translation vectors of the simulation cell lattice and the $\{\mathbf{r}_i\}$ denote the positions of the N electrons in the cell. The potential $v(\mathbf{r})$ has the periodicity of the set $\{\mathbf{t}^p\}$ of primitive translation vectors of the crystal lattice.

Now define a single-particle Hamiltonian \hat{H}_0^i consisting of the kinetic energy and external potential operators for a single electron in the many-body system. Both \hat{H}_0^i and the HF or KS DFT Hamiltonian giving the single-particle orbitals are invariant under the same set of symmetry operations, namely the set of one-electron coordinate transformations $\{T\} = \{\mathbf{R}_n | \mathbf{t}_n + \mathbf{t}^p\}$ of the crystalline space group $\mathcal{G}[\hat{H}_0^i]$. Next consider the noninteracting many-particle Hamiltonian $\hat{H}_0 = \sum_i \hat{H}_0^i$. This is invariant under a group $\mathcal{G}[\hat{H}_0]$ of operations that are tensor products of N elements of $\mathcal{G}[\hat{H}_0^i]$. For example, if \hat{H}_0 contains three electrons with labels i, j, k and each has associated with it a set of coordinate transformation such as $\{T_i\}$, then the group $\mathcal{G}[\hat{H}_0]$ consists of all possible products $T_i T_j T_k$.

The reduction in symmetry due to the interelectron Coulomb term \hat{V}_{ee} means that the interacting Hamiltonian \hat{H} in

Eq. (1) is invariant only when the same operation is applied to all electrons simultaneously. In the above example, the group of tensor product operations forming $\mathcal{G}[\hat{H}]$ would thus be restricted to those with $T_i = T_j = T_k$. Evidently \hat{H} is also invariant under translations of any one electron by a supercell lattice vector \mathbf{t}^s . Such operations are not relevant in any discussion of degeneracy classification, however, and will not be considered to be part of the group $\mathcal{G}[\hat{H}]$ in what follows. If defined in this way, the group $\mathcal{G}[\hat{H}]$ is a proper subgroup of $\mathcal{G}[\hat{H}_0]$ and is isomorphic to $\mathcal{G}[\hat{H}_0^i]$.

The trial many-electron wave functions used in our QMC calculations are of the Slater-Jastrow type,

$$\Phi_T(\mathbf{r}_1, \dots, \mathbf{r}_N) = D^\uparrow(\mathbf{r}_1, \dots, \mathbf{r}_{N_\uparrow}) D^\downarrow(\mathbf{r}_{N_\uparrow+1}, \dots, \mathbf{r}_N) \times \exp\left(\sum_{i=1}^N \chi(\mathbf{r}_i) - \sum_{i < j} u(r_{ij})\right), \quad (2)$$

where D^\uparrow and D^\downarrow are up-spin and down-spin determinants of single-particle orbitals and there are $N = N_\uparrow + N_\downarrow$ electrons. The determinants are multiplied by a Jastrow factor that contains a one-body χ function invariant under all coordinate transformations of the group $\mathcal{G}[\hat{H}_0^i]$ and a spherically symmetric two-body correlation factor u .

The product of the up-spin and down-spin determinants (call it D) of the Slater-Jastrow function transforms as a basis function of some irreducible (barring accidental degeneracies) representation $\Gamma_{\mathcal{G}[\hat{H}_0^i]}$ of the noninteracting many-particle Hamiltonian, since it is an eigenstate of the full HF or KS DFT local-density approximation (LDA) Hamiltonian which has the same symmetry group. This representation may be decomposed in terms of the irreducible representations of the subgroup $\mathcal{G}[\hat{H}]$:

$$\Gamma_{\mathcal{G}[\hat{H}_0^i]} = \Gamma_{\mathcal{G}[\hat{H}]}^1 \oplus \Gamma_{\mathcal{G}[\hat{H}]}^2 \oplus \dots \oplus \Gamma_{\mathcal{G}[\hat{H}]}^M. \quad (3)$$

The determinant may then be written as a linear combination of determinants with these definite symmetries:

$$D = \sum_{mn} a_n^m D_n^m, \quad (4)$$

where D_n^m transforms as the n th row of the representation $\Gamma_{\mathcal{G}[\hat{H}]}^m$.

Since the Jastrow factor $\exp[J]$ is invariant under all operations in $\mathcal{G}[\hat{H}]$ the functions $D_n^m \exp[J]$ are basis functions of the irreducible representations of this group. The unsymmetrized function $D \exp[J]$ is in general a basis function of a reducible representation of $\mathcal{G}[\hat{H}]$, while D itself is a basis function of an irreducible representation of $\mathcal{G}[\hat{H}_0^i]$. Since $\mathcal{G}[\hat{H}]$ is isomorphic to $\mathcal{G}[\hat{H}_0^i]$, each representation and basis function of $\mathcal{G}[\hat{H}]$ can be labeled in terms of a representation and basis function of $\mathcal{G}[\hat{H}_0^i]$. Thus one can use the labels that denote the transformation properties of the single-particle orbitals to denote how each many-electron Slater-Jastrow wave function $D_n^m \exp[J]$ transforms under the operations of $\mathcal{G}[\hat{H}]$. We now discuss the nature of these labels.

The orbitals in the determinant are Bloch functions, each with an associated wave vector \mathbf{k} . In the preliminary HF KS DFT calculation the orbitals are calculated on a Monkhorst-Pack grid in reciprocal space defined by

$$\mathbf{k} = \mathbf{k}_s + \sum_{i=1}^3 \left(\frac{l_i}{n_i}\right) \mathbf{K}_i \quad (0 \leq l_i \leq n_i - 1), \quad (5)$$

where the \mathbf{K}_i are the fundamental vectors of the reciprocal lattice and l_i and n_i are integers. The total number of sampling points is $N = n_1 \times n_2 \times n_3$. The fractional displacement \mathbf{k}_s is often taken to be zero (this will be our choice in the following) though different choices can lead to more efficient sampling nets and reduction of finite size effects in QMC.¹⁰ In general, a determinant of single-particle orbitals whose \mathbf{k} vectors lie on such a mesh forms a many-particle wave function for an $n_1 \times n_2 \times n_3$ simulation cell with an associated simulation cell wave vector, \mathbf{k}_s , equal to the offset of the mesh from the origin.¹⁰

In the general single-particle case we denote by $\phi_{ij}^{kp}(\mathbf{r})$ [$t = 1, 2, \dots, M(\mathbf{k})$, and $j = 1, 2, \dots, d_p$] the set of basis functions of the unitary irreducible representation Γ^{kp} of the space group \mathcal{G} , where $M(\mathbf{k})$ is the number of vectors in the star of \mathbf{k} generated from \mathbf{k} by rotations \mathbf{R}_t , and d_p is either the dimension of the p th unitary irreducible representation of the point group of \mathbf{k} , $\mathcal{G}_0(\mathbf{k})$ (when $\mathcal{G}[\hat{H}_0^i]$ is a symmorphic group) or the dimension of the p th relevant irreducible representation of the group of the allowed wave vector \mathbf{k} , $\mathcal{G}(\mathbf{k})$ (when $\mathcal{G}[\hat{H}_0^i]$ is nonsymmorphic). Then (a) $\phi_{ij}^{kp}(\mathbf{r})$ is a Bloch function with wave vector $\mathbf{R}_t \mathbf{k}$, and (b) the functions $\phi_{ij}^{kp}(\mathbf{r})$ ($j = 1, 2, \dots, d_p$) form a basis for the unitary irreducible representation of $\mathcal{G}_0(\mathbf{k})$ when $\mathcal{G}[\hat{H}_0^i]$ is a symmorphic group or a basis for the relevant irreducible representation of $\mathcal{G}(\mathbf{k})$ when $\mathcal{G}[\hat{H}_0^i]$ is a nonsymmorphic group.

Since the group of the full many-electron Hamiltonian $\mathcal{G}[\hat{H}]$ is isomorphic to $\mathcal{G}[\hat{H}_0^i]$, each eigenstate of \hat{H} and each of the many-electron states previously labeled $\Psi_n^m = D_n^m \exp[J]$ can thus be labeled in terms of the single-particle labels $\Psi_{ij}^{kp}(\mathbf{r}_1, \mathbf{r}_2, \dots, \mathbf{r}_N)$ using the standard notation in which the representation kp corresponds to m and the row tj corresponds to n .

B. Symmetry properties of excited determinants

For any symmetry operation T of the group $\mathcal{G}[\hat{H}]$, the action of the corresponding scalar transformation operator $P(T)$ on a determinant D_m is given by

$$P(T)D_m = \sum_{n=1}^d \Gamma_{nm}(T)D_n, \quad (6)$$

where, for the example of the $\Gamma_{25'v} \rightarrow \Gamma_{15c}$ transition in diamond considered earlier, the dimension d is nine and the representation Γ_{nm} is reducible. Since the D_n form an orthonormal set, the matrix whose elements are

$$\Gamma_{nm}(T) = \int D_n^* P(T) D_m \, d\tau \quad (7)$$

is unitary.

TABLE I. Decompositions into irreducible representations of possible excitations in diamond.

Excitation
$\Gamma_{1v} \rightarrow \Gamma_{2'c} = \Gamma_{2'}$
$\Gamma_{1v} \rightarrow \Gamma_{15c} = \Gamma_{15}$
$\Gamma_{1v} \rightarrow L_{1c} = L_1$
$\Gamma_{1v} \rightarrow X_{1c} = X_1$
$\Gamma_{25'v} \rightarrow L_{3c} = L_1 \oplus L_2 \oplus 2L_3$
$\Gamma_{25'v} \rightarrow \Gamma_{15c} = \Gamma_{2'} \oplus \Gamma_{12'} \oplus \Gamma_{15} \oplus \Gamma_{25}$
$\Gamma_{25'v} \rightarrow L_{1c} = L_1 \oplus L_3$
$\Gamma_{25'v} \rightarrow X_{1c} = X_1 \oplus X_3 \oplus X_4$
$X_{1v} \rightarrow \Gamma_{15c} = X_1 \oplus X_3 \oplus X_4$
$X_{1v} \rightarrow X_{1c} = X_1 \oplus X_2 \oplus X_3 \oplus X_4 \oplus \Gamma_1 \oplus \Gamma_{12} \oplus \Gamma_{25'} \oplus \Gamma_{2'} \oplus \Gamma_{12'} \oplus \Gamma_{15}$
$X_{4v} \rightarrow \Gamma_{15c} = X_1 \oplus X_2 \oplus X_3$
$X_{4v} \rightarrow \Gamma_{2'c} = X_3$
$X_{4v} \rightarrow L_{1c} = L_2 \oplus L_3 \oplus L_{2'} \oplus L_{3'}$
$X_{4v} \rightarrow X_{1c} = X_1 \oplus X_2 \oplus X_3 \oplus X_4 \oplus \Gamma_{15'} \oplus \Gamma_{25'} \oplus \Gamma_{15} \oplus \Gamma_{25}$
$L_{2'v} \rightarrow L_{3c} = X_1 \oplus X_2 \oplus X_3 \oplus X_4 \oplus \Gamma_{12} \oplus \Gamma_{15'} \oplus \Gamma_{25'}$
$L_{2'v} \rightarrow \Gamma_{15c} = L_1 \oplus L_3$
$L_{1v} \rightarrow L_{3c} = X_1 \oplus X_2 \oplus X_3 \oplus X_4 \oplus \Gamma_{12'} \oplus \Gamma_{15} \oplus \Gamma_{25}$
$L_{1v} \rightarrow \Gamma_{15c} = L_{2'} \oplus L_{3'}$
$L_{1v} \rightarrow L_{1c} = X_1 \oplus X_3 \oplus \Gamma_1 \oplus \Gamma_{25'}$
$L_{3'v} \rightarrow \Gamma_{2'c} = L_3$
$L_{3'v} \rightarrow L_{3c} = 2X_1 \oplus 2X_2 \oplus 2X_3 \oplus 2X_4 \oplus \Gamma_{1'} \oplus \Gamma_{2'} \oplus \Gamma_{12'} \oplus 2\Gamma_{15} \oplus 2\Gamma_{25}$
$L_{3'v} \rightarrow \Gamma_{15c} = L_1 \oplus L_2 \oplus 2L_3$
$L_{3'v} \rightarrow L_{1c} = X_1 \oplus X_2 \oplus X_3 \oplus X_4 \oplus \Gamma_{12'} \oplus \Gamma_{15} \oplus \Gamma_{25}$
$L_{3'v} \rightarrow X_{1c} = L_1 \oplus L_2 \oplus 2L_3 \oplus L_{1'} \oplus L_{2'} \oplus 2L_{3'}$

Transformation of an excited state function $\Psi = D_m \exp[J]$ gives

$$P(T)D_m \exp[J] = \sum_{n=1}^d \Gamma_{nm}(T)D_n \exp[J], \quad (8)$$

where in general $\Gamma_{nm}(T)$ is reducible. To decompose the reducible representation of the arbitrarily excited determinant into its constituent irreducible representations as in Eq. (3), we first require an expression giving the character system of the reducible representation. This may be obtained by evaluating the trace of the $\Gamma(T)$ matrices for each class of symmetry operator as follows.

Consider the Slater matrix for each spin component, where each row corresponds to a different single-particle orbital and each column to a different electron position. Application of a scalar transformation operator $P(T)$ transforms each single-particle orbital in the matrix into a linear combination of the orbitals in its degenerate set with coefficients $\Gamma_{ij}^{kp}(T)$. Using the definition of the determinant one can expand the transformed determinant into a sum of determinants of orbitals. Noting that all of these determinants vanish except those containing a different orbital in each row, one can show that the ground state in diamond with $\mathbf{k}_s = \mathbf{0}$ transforms as follows, where each determinant D^\uparrow and D^\downarrow in Eq. (2) consists of the same closed shell of orbitals:

$$P(T)D^{\uparrow,\downarrow} = \prod_{\substack{\text{occupied} \\ \mathbf{k}p}} \det[\Gamma^{kp}(T)]D^{\uparrow,\downarrow}. \quad (9)$$

Since the determinant, $\det[\Gamma^{kp}(T)]$, of each matrix representation is a real number for a $2 \times 2 \times 2$ simulation cell in diamond the ground-state Slater-Jastrow function $\Psi_G = D^\uparrow D^\downarrow \exp[J]$ is invariant under all operations of the group and thus belongs to the identity representation $\Gamma^{\mathbf{k}=0,p=1}$.

To construct an excited-state wave function one of the ground-state valance orbitals is replaced in, say, D^\uparrow with a conduction orbital. One can show in this case that the character of the reducible representation in Eq. (7) for diamond is

$$\chi(T) = \chi_{hole}^*(T) \chi_{electron}(T). \quad (10)$$

The ‘‘hole’’ subscript refers to the characters of the irreducible representation of the single-particle valance orbital ($\Gamma_{25'}$ for the simple example) that is excited to a virtual orbital (e.g. Γ_{15}) with its corresponding characters denoted by the ‘‘electron’’ subscript. There are well-established procedures for finding the characters of the irreducible representations of the nonsymmorphic space group of the diamond structure (detailed for example, on pp. 242–245 of Ref. 12). Having thus derived the character system of the reducible representation, it may be decomposed into its irreducible components following the usual prescription. For the case at hand, the decomposition is $\Gamma_{2'} \oplus \Gamma_{12'} \oplus \Gamma_{15} \oplus \Gamma_{25}$ where the standard notation¹¹ for the irreducible representations has been used (see, e.g., Table D.2 Ref. 12). Table I lists all such decompositions of the representations for each of the excitations in diamond considered in this paper, derived from a straightforward but tedious computation of each term in Eq. (10).

To determine the correct linear combinations of determinants that give wave functions $\Psi_{ij}^{kp}(\mathbf{r}_1, \mathbf{r}_2, \dots, \mathbf{r}_N)$ of a definite symmetry we apply the projector

$$\left(\frac{d_p}{g}\right) \sum_{T \in \mathcal{G}} \chi^p(T) * P(T) \quad (11)$$

to each of the possible determinant states. In performing this operation in diamond we need only consider the smaller determinant composed of orbitals from the partially occupied valence state from which the electron was removed and the partially occupied conduction state into which the electron was added. For example, for the $\Gamma_{25'v} \rightarrow \Gamma_{15c}$ calculation each of the states is threefold degenerate so one needs to apply a projector (for each of the four different symmetries) to a 3×3 determinant, composed of two valence orbitals and a conduction orbital.

C. Level splitting

For determinants D_m that transform among themselves as in Eq. (6) the expectation value

$$\langle D_m \exp[J] | \hat{H}_0 | D_m \exp[J] \rangle = E_0 \quad (12)$$

is independent of the hole and particle orbitals used to form these excited determinants. When the interacting Hamiltonian of Eq. (1) replaces \hat{H}_0 in these expressions a splitting arises from the interelectron Coulomb term; its magnitude is determined by

$$\left\langle D_m \exp[J] \left| \sum_{i>j} \frac{1}{|\mathbf{r}_i - \mathbf{r}_j|} \right| D_m \exp[J] \right\rangle.$$

The use of arbitrary mixed symmetry orbitals in the trial function will thus produce an essentially random shift away from the true energy. Here we show that the maximum shift is produced using the symmetrized trial functions that transform according to the appropriate irreducible representations.

Any arbitrary normalizable function can be decomposed into a linear combination of basis functions of the irreducible representations of the group $\mathcal{G}[\hat{H}]$ of the Schrödinger equation. We therefore write the many-body wave function Ψ as

$$\Psi = \sum_p \sum_{m=1}^{d_p} a_m^p \Psi_m^p, \quad (13)$$

where Ψ_m^p is some function transforming as the m th row of the unitary irreducible representation Γ^p . Let Ψ_m^p and Ψ_n^q be, respectively, basis functions for the unitary irreducible representations Γ^p and Γ^q of the space group. The expectation value of the Hamiltonian is then

$$E = \sum_p \sum_{m=1}^{d_p} \sum_q \sum_{n=1}^{d_q} a_m^{p*} a_n^q \langle \Psi_m^p | \hat{H} | \Psi_n^q \rangle. \quad (14)$$

Assuming Γ^p and Γ^q are inequivalent if $p \neq q$, but are identical if $p = q$, the Wigner-Eckart theorem may be used to show that

$$\langle \Psi_m^p | \hat{H} | \Psi_n^q \rangle = E_p \delta_{pq} \delta_{mn}. \quad (15)$$

Hence

$$E = \sum_p E_p \sum_{m=1}^{d_p} |a_m^p|^2 = \sum_p |A^p|^2 E_p, \quad (16)$$

where $\sum_p |A^p|^2 = \sum_p \sum_{m=1}^{d_p} |a_m^p|^2 = 1$. Thus for any arbitrary normalizable function its expectation value is bounded by

$$\min_p E_p \leq E \leq \max_p E_p, \quad (17)$$

where the energy can equal one of the bounds typically when the wave function transforms as a basis function of an irreducible representation.

It is not clear *a priori* whether the splitting is large enough to warrant the extra computational effort that is evidently required to take account of it (say, by computing excitations involving all nine determinants and performing some sort of average). One could justify neglecting such measures if one knew the maximum possible splitting was sufficiently small relative to the attainable error bars on the excitation energies.

This is the end of the story for the VMC case. The DMC case is somewhat more complicated, since the use of the fixed-node approximation may further split each state if the trial wave function has a definite symmetry $\Psi_{ij}^{kp}(\mathbf{r}_1, \mathbf{r}_2, \dots, \mathbf{r}_N)$, and transforms according to an irreducible representation of dimension greater than one, such as when $\mathbf{k} = X$ and $p = 1$. The nodal surface of the trial function will evidently depend on j (the row of the irreducible representation), and hence so may the DMC energy, as the DMC algorithm may break the symmetry of the trial wave function in this case. This effect is obviously absent if $\mathbf{k}p$ corresponds to a one-dimensional representation such as $\Gamma^{\mathbf{k}=0, p=1}$.

D. Variational principles

For the VMC case, using a wave function with a definite symmetry $\Psi_{ij}^{kp}(\mathbf{r}_1, \mathbf{r}_2, \dots, \mathbf{r}_N)$ the VMC energy is an upper bound to the lowest exact energy with that same symmetry. Consider, for example, the decomposition

$$\Gamma_{25'v} \rightarrow X_{1c} = X_1 \oplus X_3 \oplus X_4. \quad (18)$$

Forming a VMC state with symmetry X_3 (say) will give a VMC energy that is an upper bound to the lowest exact energy state of symmetry X_3 .

In diamond with a $2 \times 2 \times 2$ simulation cell a variational principle applicable to the DMC method will apply to (1) the ground state, (2) the lowest energy state of each trial wave function of a definite symmetry $\Psi_{ij}^{kp}(\mathbf{r}_1, \mathbf{r}_2, \dots, \mathbf{r}_N)$ when $\mathbf{k} = 0$ (Γ point) and p corresponds to a one-dimensional representation such as Γ_1 , and (3) the lowest energy state with a definite $\mathbf{k} = X$ or $\mathbf{k} = L$, because of a weaker variational principle,⁹ since the group of translations contains only one-dimensional irreducible representations and is a subgroup of $\mathcal{G}[\hat{H}]$. So wave functions that transform as (say) X_1, X_2, X_3 , or X_4 with a definite \mathbf{k} are all bounded below by the same lowest energy of an exact state with a definite $\mathbf{k} = X$. Obviously the DMC variational principle has far less utility than the VMC variational principle.

TABLE II. Excitation energies of diamond in eV.

Excitation	DMC ^a	<i>GW</i> ^b	<i>GW</i> ^c	LDA ^b	Expt ^d
$\Gamma_{1v} \rightarrow \Gamma_{15c}$	32.18	30.51	30.5	26.93	-
$\Gamma_{1v} \rightarrow \Gamma_{2'c}$	41.05	37.42	37.8	34.45	-
$\Gamma_{1v} \rightarrow L_{1c}$	35.79	33.51	-	29.74	-
$\Gamma_{1v} \rightarrow X_{1c}$	30.69	29.18	-	25.98	-
$\Gamma_{25'v} \rightarrow \Gamma_{15c}$	7.13	7.63	7.5	5.58	7.3
$\Gamma_{25'v} \rightarrow L_{1c}$	10.16	10.23	-	8.76	-
$\Gamma_{25'v} \rightarrow X_{1c}$	5.71	6.30	-	4.63	-
$X_{1v} \rightarrow X_{1c}$	20.49	20.10	-	17.24	-
$X_{4v} \rightarrow \Gamma_{15}$	14.41	14.32	-	11.84	-
$X_{4v} \rightarrow L_{1c}$	17.08	17.32	-	14.54	-
$X_{4v} \rightarrow X_{1c}$	12.70	12.99	-	10.89	12.5, 12.6
$X_{4v} \rightarrow X_{4c}$	26.90	26.19	-	23.17	-
$L_{2'v} \rightarrow L_{1c}$	27.94	27.58	-	23.90	-
$L_{1v} \rightarrow L_{1c}$	25.13	24.9	-	21.72	-
$L_{3'v} \rightarrow \Gamma_{15c}$	10.78	10.61	-	8.36	-
$L_{3'v} \rightarrow X_{4c}$	22.41	22.48	-	19.69	-
$L_{3'v} \rightarrow L_{1c}$	13.32	13.61	-	11.17	12.5, 16.3
$L_{3'v} \rightarrow L_{2'c}$	22.03	21.12	-	18.45	24.0

^aThis work. The statistical error bars on the DMC energies are ± 0.2 eV.

^bReference 18.

^cReference 19.

^dExperimental values taken from the compilation given in Ref. 21.

V. QMC CALCULATIONS

In this section we give some brief practical details of our diamond QMC calculations. The electron-ion potential v_α was modeled by a norm-conserving Trouiller-Martins LDA pseudopotential. The infinite summation of interparticle Coulomb interactions in the periodic system can be handled with the usual Ewald interaction potential but only at the cost of potentially large finite-size errors. An alternative approach is to use our recently introduced “model periodic Coulomb interaction,” which greatly reduces such errors.¹³ In excitation calculations the choice of interaction potential is less important since the finite-size error largely cancels when taking the difference of excited- and ground-state energies,⁶ and for simplicity we have chosen to use the Ewald interaction in this study. We used an fcc simulation cell built from a $2 \times 2 \times 2$ array of primitive cells, subject to periodic boundary conditions and containing 16 carbon pseudoatoms and 64 electrons.

The Slater determinants were constructed from single-particle orbitals obtained from an LDA calculation using the correlation functional of Ceperley and Alder¹⁴ as parametrized by Perdew and Zunger.¹⁵ The LDA orbitals were computed using the program¹⁶ CRYSTAL95 at the Γ point of the simulation-cell Brillouin zone using an atom-centered Gaussian basis set. The basis set was made up of four uncontracted sp functions and one d polarization function per pseudoatom, with exponents optimized in the perfect solid.¹⁷ Although the Γ -point scheme does not give optimal Brillouin zone sampling,¹⁰ it does preserve the full symmetry of the system and allows comparison with a wider number of established results. The Γ point of the simulation-cell Brillouin zone unfolds to three inequivalent \mathbf{k} points in the primitive

Brillouin zone. These are (0,0,0) (the Γ point), $(0,0,\frac{1}{2})2\pi/a$ (the X point), and $(\frac{1}{2},\frac{1}{2},\frac{1}{2})2\pi/a$ (the L point).

The χ function used in our Jastrow factor has the full symmetry of the diamond structure and is expressed as a Fourier series containing 16 inequivalent parameters. We used spherically symmetric parallel and antiparallel spin u functions, which satisfy the electron-electron cusp conditions and contain a total of eighteen parameters. The optimized parameter values were obtained by minimizing the variance of the energy.

VI. EXCITED-STATE ENERGY RESULTS

Diffusion Monte Carlo simulations were performed for 18 separate promotion excitations involving orbitals at the $\Gamma, X,$ and L wave vectors in diamond. In these initial calculations, promotions involving sets of degenerate orbitals were modeled using the unsymmetrized orbitals obtained directly from CRYSTAL95. Our calculated excitation energies are shown in Table II together with the results of comparable GW and LDA calculations.^{18,19} The GW method is known to give extremely good results for weakly correlated systems such as diamond, and the various GW calculations are seen to be in excellent agreement with one another. The experimental data are quite sparse, but where available they are in reasonable agreement with the GW data. The LDA data show the well-known underestimation of the excitation energies. For the low energy excitations the DMC energies are a little too small, while for larger excitation energies they are too large. Nevertheless the agreement between the DMC results and the GW data is very encouraging.

To obtain DMC band energies from the 18 excitation en-

TABLE III. Band energies of diamond in eV.

Band	DMC ^a	GW ^b	GW ^c	LDA ^b	HF ^a	Expt. ^d
$\Gamma_{2'c}$	15.83	14.54	14.8	13.10	24.87	15.3 ± 0.5
Γ_{15c}	7.23	7.63	7.5	5.58	14.46	7.3
$\Gamma_{25'v}$	0.0	0.0	0.0	0.0	0.0	0.0
Γ_{1v}	-25.22	-22.88	-23.0	-21.35	-29.19	$-24.2 \pm 1, -21 \pm 1, -23.0 \pm 0.2$ ^e
X_{4c}	19.48	19.5	-	16.91	29.63	-
X_{1c}	5.58	6.3	-	4.63	13.42	-
X_{4v}	-7.15	-6.69	-	-6.26	-8.41	-
X_{1v}	-14.91	-13.8	-	-12.61	-17.73	-
$L_{2'c}$	18.83	18.14	17.9	15.67	27.61	20 ± 1.5
L_{3c}	-	10.23	-	8.76	18.51	-
L_{1c}	10.19	10.63	-	8.39	18.32	-
$L_{3'v}$	-3.20	-2.98	-	-2.78	-3.80	-
L_{1v}	-14.94	-14.27	-14.4	-13.33	-17.90	-12.8 ± 0.3
$L_{2'v}$	-17.75	-16.95	-17.3	-15.51	-21.88	-15.2 ± 0.3

^aThis work. The statistical error bars on the DMC energies are ± 0.2 eV.

^bReference 18.

^cReference 19.

^dExperimental values taken from the compilation given in Ref. 18, except for the footnote e value.

^eExperimental value taken from Ref. 20.

ergies E_{DMC}^{ij} in Table II (which correspond to transitions between seven valence and six conduction band energy levels ϵ_i), we performed a least squares fit to the DMC data. This was done by minimizing $\Sigma[E_{DMC}^{ij} - (\epsilon_i - \epsilon_j)]^2$ with respect to the ϵ_i , where the sum is over the 18 promotion excitations. The resulting band energies may be compared with the experimental data and equivalent GW/LDA numbers in Table III. For greater clarity the DMC and GW band energies are also plotted in Fig. 1 together with the results of an LDA band structure calculation to guide the eye. The energies at the top of the valence band have been aligned. The DMC band energies around the gap region are in good agreement with the GW and experimental data, but consistently lie slightly below them in the lower part of the valence band.

In our previous work on excitation energies in silicon,⁶ we performed an analysis of the fraction of correlation energy recovered by the DMC simulation. This percentage was found to decrease slowly with increasing excitation energy. However, because the magnitude of the correlation contribution increases rapidly with increasing excitation energy the DMC higher excitation energies were somewhat too large. This analysis indicated that the residual errors in the DMC excitation energies are mostly due to the errors in the nodal surfaces of the excited-state guiding wave functions rather than in the ground state. These conclusions apply equally well in the present case of diamond.

VII. SPLITTING RESULTS

Here we investigate the energy splitting for the direct excitation of an electron across the band gap of diamond at the Γ point. The hole orbital is one of the triply degenerate

single-particle orbitals at the top of the valence band with $\mathbf{k}=(0,0,0)$. Under the symmetry operations of the crystal in diamond, a Bloch orbital transforms as a representation Γ^{kp} of O_h . The hole orbitals at the valence band edge in fact transform as the $\Gamma_{25'}$ representation of O_h , according to the standard notation.¹² The electron is excited into one of the triply degenerate orbitals at the bottom of the conduction band. These transform as the Γ_{15} representation of O_h .

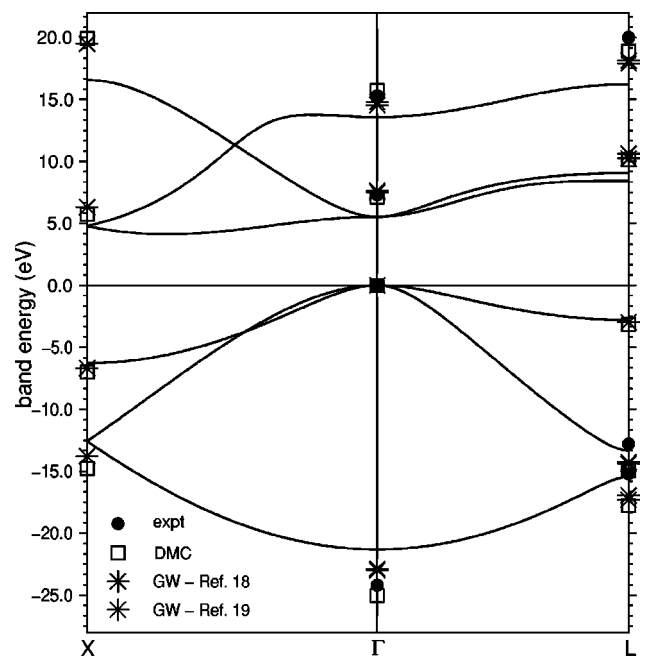


FIG. 1. The DMC band structure compared with GW and experimental data, overlaid with an LDA band structure.

There are a total of nine determinants that may be formed with this set of orbitals, and these determinants form a set of basis functions for a reducible representation of the space group. As noted in Sec. IV B, this reducible representation decomposes to $\Gamma_{2'} \oplus \Gamma_{12'} \oplus \Gamma_{15} \oplus \Gamma_{25}$.

The VMC excitation energy results for the $\Gamma_{25'v} \rightarrow \Gamma_{15c}$ transition using the nine possible wave functions derived from the mixed symmetry orbitals produced by the CRYSTAL code were 7.04, 7.05, 7.07, 7.08, 7.10, 7.11, 7.30, 7.32, 7.35 eV \pm 0.08 eV (average 7.16). The four correctly symmetrized wave functions gave excitation energies of 6.98, 7.06, 7.14, and 7.18 eV \pm 0.08 eV (average 7.09 eV) (for Γ_{25} , $\Gamma_{12'}$, Γ_{15} , and $\Gamma_{2'}$, respectively).

DMC calculations of the same excitation energies gave 6.69, 6.75, 6.84, 6.99, 7.00, 7.18, 7.21, 7.28, and 7.48 eV \pm 0.2 eV (average 7.05 eV) in the unsymmetrized cases. As mentioned earlier, the fixed-node approximation used in the DMC calculation breaks the degeneracy between the different rows of the multidimensional representations. The symmetrized DMC results were 6.73, 6.80, and 7.48 eV (for the three rows of Γ_{25}), 7.02 and 7.07 eV (for $\Gamma_{12'}$), 6.85, 7.00, and 7.14 eV (for Γ_{15}), and 7.25 eV (for $\Gamma_{2'}$) again with an error bar of \pm 0.2 eV. This fixed-node splitting is thus comparable in magnitude to the splitting observed in the unsymmetrized case.

The first point to note is that on average these numbers agree very well with the experimental number of 7.3 eV, given that we expect our calculated energy to be lowered slightly by the exciton binding energy arising from the interaction between electron and hole. In both VMC and DMC cases the difference between the lowest and the highest energies using the unsymmetrized single determinants is around four times the size of the error bar. This demonstrates the importance of the level splitting effect in QMC calculations of excitation energies. In the calculations performed here, the magnitude of the splitting observed with the symmetrized trial functions is not significantly different from

that using the unsymmetrized single determinants. The largest and smallest VMC energies do not explicitly emerge from the symmetrized calculations as predicted by the theory of Sec. IV C, but the statistical error bars are too large for this to be of significance.

VIII. CONCLUSIONS

The DMC method provides a unified framework for calculating accurate ground- and excited-state energies. The fixed-node approximation works to our advantage by preventing variational collapse to lower energy states of the same symmetry, allowing calculations of both direct and indirect excitations. The accuracy of the excited-state energies is determined by the quality of the nodal surfaces of the guiding wave functions. In the case of diamond, good agreement was found between DMC and the available *GW* and experimental data. The problem of level splitting arises in calculations involving a many-particle trial function built from arbitrary degenerate single-particle orbitals. We have performed a group theoretical analysis of this effect, and have shown using actual numerical simulations that it is significant for the case of diamond. Using symmetrized trial wave functions with determinants composed of single-particle orbitals obtained from an LDA calculation, we find that the fixed-node approximation introduces a splitting comparable in magnitude to this level splitting in diamond. We have further amplified the nature of variational principles in QMC calculations of excited states.

ACKNOWLEDGMENTS

Financial support was provided by the Engineering and Physical Sciences Research Council (U.K.). Our calculations are performed on the CRAY-T3E computer at the Edinburgh Parallel Computing Center, and on the Hitachi SR2201 computer at the Cambridge HPCF.

*Present address: Lawrence Livermore National Laboratory, Livermore, California 94550.

¹W.L. McMillan, Phys. Rev. **138**, A442 (1965); D. Ceperley, G.V. Chester, and M.H. Kalos, Phys. Rev. B **16**, 3081 (1977).

²D. M. Ceperley and M. H. Kalos, in *Monte Carlo Methods in Statistical Physics*, edited by K. Binder (Springer, Berlin, 1979); K. E. Schmidt and M. H. Kalos, in *Monte Carlo Methods in Statistical Physics II*, edited by K. Binder (Springer, Berlin, 1984).

³R.M. Grimes, B.L. Hammond, P.J. Reynolds, and W.A. Lester, Jr., J. Chem. Phys. **85**, 4749 (1986).

⁴L. Mitáš, in *Computer Simulation Studies in Condensed Matter Physics V*, edited by D. P. Landau, K. K. Mon, and H. B. Schuttler (Springer, Berlin, 1993).

⁵L. Mitáš and R.M. Martin, Phys. Rev. Lett. **72**, 2438 (1994).

⁶A.J. Williamson, R.Q. Hood, R.J. Needs, and G. Rajagopal, Phys. Rev. B **57**, 12 140 (1998).

⁷E. Hylleraas and B. Undheim, Z. Phys. **65**, 759 (1930); J.K.L. Macdonald, Phys. Rev. **43**, 830 (1933).

⁸J.B. Anderson, J. Chem. Phys. **65**, 4121 (1976).

⁹W.M.C. Foulkes, R.Q. Hood, and R.J. Needs, Phys. Rev. B **60**, 4558 (1999).

¹⁰G. Rajagopal, R.J. Needs, A. James, S. Kenny, and W.M.C. Foulkes, Phys. Rev. B **51**, 10 591 (1995).

¹¹L.P. Bouckaert, R. Smoluchowski, and E.P. Wigner, Phys. Rev. **50**, 58 (1936).

¹²J. F. Cornwell, *Group Theory in Physics* (Academic Press, 1994), Vol. 1.

¹³P.R.C. Kent, R.Q. Hood, A.J. Williamson, R.J. Needs, W.M.C. Foulkes, and G. Rajagopal, Phys. Rev. B **59**, 1917 (1999).

¹⁴D.M. Ceperley and B.I. Alder, Phys. Rev. Lett. **45**, 566 (1980).

¹⁵J.P. Perdew and A. Zunger, Phys. Rev. B **23**, 5048 (1981).

¹⁶R. Dovesi, V. R. Saunders, C. Roetti, M. Causà, N. M. Harrison, R. Orlando, and E. Aprà, *CRYSTAL95 User Manual* (University of Torino, Torino, 1996).

¹⁷M. D. Towler, TCM Gaussian Basis Set Library (1997), <http://www.tcm.phy.cam.ac.uk/~mdt26/crystal.html>

¹⁸M. Rohlfing, P. Krüger, and J. Pollmann, Phys. Rev. B **48**, 17 791 (1993).

¹⁹M.S. Hybertsen and S.G. Louie, Phys. Rev. B **34**, 2920 (1986).

²⁰I. Jiménez, L.J. Terminello, D.G.J. Sutherland, J.A. Carlisle, E.L. Shirley, and F.J. Himpsel, Phys. Rev. B **56**, 7215 (1997).

²¹*Landolt-Börnstein Numerical Data and Functional Relationships in Science and Technology*, edited by O. Madelung (Springer, Berlin, 1982), Vol. 17, p. 36.